

## Influences of multi-factors on Corrosion Resistance of TA2 pure Titanium in Brine Solution Produced from Vacuum Salt Plant

Xuedan Chen<sup>1,2</sup>, Qingshan Fu<sup>2</sup>, Min Gong<sup>2</sup>, Wenheng Huang<sup>2</sup>, Zuxiao Yu<sup>2</sup>,  
Qilong Liao<sup>1,\*</sup>

<sup>1</sup> School of Materials Science and Engineering, Southwest University of Science and Technology, Mianyang 621010, PR China

<sup>2</sup> Key Laboratory of Material Corrosion and Protection of Sichuan Province, Zigong 643000, China

\*E-mail: [sendysan@126.com](mailto:sendysan@126.com); [lql343@163.com](mailto:lql343@163.com)

Received: 22 February 2022 / Accepted: 23 March 2022 / Published: 7 May 2022

---

In vacuum salt industry, water in brine is evaporated in evaporators for harvest of salt crystals. Considering the harsh corrosion environment in brine, titanium and its alloy are widely used in the pipes and evaporators. Here, we systematically evaluate the effects of kinds of factors including concentrations of  $\text{CO}_3^{2-}$  and  $\text{S}^{2-}$  in the brine, pH value and flowing rate of the brine on the corrosion behaviors of pure titanium (TA2) by electrochemical methods. The results show that with the increase of concentration of  $\text{CO}_3^{2-}$  or  $\text{S}^{2-}$ , the corrosion resistance of TA2 decreases. The rise of flowing rate aggravates the corrosion of TA2 in the brine. When the pH value of the brine is placed in the range of 7–8, TA2 presents the better corrosion resistance performance. In addition, the orthogonal experiments demonstrate that  $\text{CO}_3^{2-}$  concentration and pH value of the brine exhibit relatively greater influence on the corrosion behavior of TA2 than  $\text{S}^{2-}$  concentration and flowing rate. To acquire the better corrosion resistance in the brine, the lower concentration of  $\text{CO}_3^{2-}$  and the suitable pH range should be guaranteed.

---

**Keywords:** Titanium; Brine; Corrosion resistance; Electrochemical evaluation; Flowing rate

### 1. INTRODUCTION

Vacuum salt is a high-purity salt made by using the vacuum evaporation process, by which either fine-grained salt or rough-grained salt can be derived according to the requirement of the users. Its main procedure is that evaporating water from brine solution for salt formation. However, the brine contains various ions such as  $\text{Na}^+$ ,  $\text{Cl}^-$ ,  $\text{S}^{2-}$ ,  $\text{Mg}^{2+}$ ,  $\text{Ca}^{2+}$ , and some  $\text{CO}_3^{2-}$  (introduced for removal of some impurities in the brine), which may corrode the evaporators and pipes [1-2]. Thus, titanium is utilized in vacuum salt industry widely due to its excellent corrosion resistance [3-4].

As far as corrosion is concerned, titanium and its alloys belong to oxide-passivated metals including the stainless steels, as well as nickel, cobalt, and aluminum-based alloys. However, titanium is a special member in this group as titanium can corrode either very quickly or extremely slowly, depending on the environmental conditions. For example, titanium can endure many oxidizing acidic media, such as chromic and nitric acids and diluted sulfuric acid because of the easy formation of a highly protective oxide film which possesses high chemical stability [5], whereas some kinds of halide ions, especially the fluoride ion, can seriously deteriorate the corrosion resistance of titanium even at a low content [6].

The type and concentration of chemical ingredients, temperature, pressure, flow velocity, pH value all the parameters of media can change the corrosion behavior of titanium. For instance, in oral environment the titanium implants will be subjected to the conditions of varying pH values caused by inflammatory or other processes, which may turn the medium acidic leading to the breakdown of oxide layer formed on the metal surface and subsequent severe corrosion of implants [7-8]. Blackwood's research revealed that in the absence of CO<sub>2</sub>, Ti (grades 5) suffered crevice corrosion at temperature of 200 °C; however, crevice corrosion occur at as low as 80 °C in the presence of CO<sub>2</sub> [9]. The dynamic or static electrolyte also leads to different corrosion performances of Ti [10]. Various ions with different concentrations in media also influence the corrosion performances of titanium [11]. Fluoride ions in dilute H<sub>2</sub>SO<sub>4</sub> solution have been demonstrated that can accelerate the corrosion of titanium via changing the structure of the film formed at OCP (open circuit potential) and destroying the protectiveness of the film [12]. Fluoride ions, chloride ions, hydroxyl ions were also proved their boosting Ti corrosion, meanwhile relieved deterioration was observed when nitrate ions or sulfate ions was added in media [13-15].

Considering the complex multi-ion system in brine, the corrosion resistance of titanium may be changed according to the situation of the brine. VA Levin et al. have observed the multi-ion-coexisting system of brine caused different degrees of titanium corrosion [16]. However, there is a lack of systemic research on the influence of the parameters of brine on corrosion of titanium. So, here we evaluated the corrosion behavior of commercial pure titanium (TA2) in brine under a set of parameters such as different ion concentrations of CO<sub>3</sub><sup>2-</sup> and S<sup>2-</sup>, several pH values, flow velocity. Additionally, orthogonal experiment was applied to find out the main factors of brine controlling the corrosion of titanium.

## 2. MATERIALS AND METHODS

Pure titanium sheets were acquired from commercial route. The brine solution was fetched from a vacuum salt plant in Zigong, China, and its main chemical composition (g/L) is: Na<sup>+</sup> 117.3, Ca<sup>2+</sup> 1.69, Mg<sup>2+</sup> 0.082, SO<sub>4</sub><sup>2-</sup> 3.84, Cl<sup>-</sup> 176.3. Potassium chloride (KCl), sodium hydroxide (NaOH), sodium carbonate (Na<sub>2</sub>CO<sub>3</sub>), potassium hydroxide (KOH), hydrogen chloride (HCl), sodium sulfide nonahydrate (Na<sub>2</sub>S•9H<sub>2</sub>O), hydrogen fluoride (HF), nitric acid (HNO<sub>3</sub>), acetone, absolute ethyl alcohol, ethoxyline resin, curing agent were purchased from Chengdu Cologne Chemical Co. Ltd. Distilled water was used as required.

Commercial pure titanium sheet ( $\Phi 10\text{mm} \times 6\text{mm}$ ) was embedded in epoxy resin with an exposed area of  $0.785\text{ cm}^2$ . The exposed surface was polished through successive silicon carbide papers to 1000 grit. After that, the sample was washed with acetone and distilled water in sequence, and then dried in cold air. The dried encapsulated titanium sheet acted as the working electrode and platinum wire as the counter electrode, saturated calomel electrode (SCE) as the reference electrode. The brine solution was employed as electrolyte. The corrosion behavior of the Ti sheets was evaluated on PARSTAT2273 electrochemical workstation by testing potentiodynamic curves and electrochemical impedance spectroscopy (EIS). The scanning rate of anodic polarization of the Tafel curve was  $5\text{ mV/s}$ ; the scan rate of weakly polarization region was  $0.5\text{ mV/s}$  and the polarization range is  $-250\text{--}250\text{ mV}$  (vs. open circuit potential). The polarization resistance ( $R_p$ ) was determined from the slope of the current–potential lines obtained. The EIS tests were performed at OCP using AC signals of amplitude  $5\text{ mV}$  peak-to-peak from  $100\text{ kHz}$  to  $0.01\text{ Hz}$ . Before measurements of the polarization curves and EIS, the working electrode was immersed in the test solution at OCP for  $30\text{ min}$  to attain a stable state. To identify the effects of  $\text{CO}_3^{2-}$ ,  $\text{S}^{2-}$ , pH value on the corrosion performances, a set of concentration values of  $\text{CO}_3^{2-}$  and  $\text{S}^{2-}$  in the brine solution were achieved by adding  $\text{Na}_2\text{CO}_3$  and  $\text{Na}_2\text{S}\cdot 9\text{H}_2\text{O}$ , respectively. The pH values of the brine solution were adjusted using  $\text{NaOH}$  or  $\text{HCl}$ .

### 3. RESULTS AND DISCUSSION

#### 3.1 Influence of $\text{CO}_3^{2-}$ on corrosion behavior of TA2

According to the polarization resistance ( $R_p$ ) profile (Figure. 1a) and Tafel polarization curve (Figure. 1b) of the titanium working electrode in the brine solution with concentrations of  $\text{CO}_3^{2-}$  ( $0\text{--}3.5\text{ g/L}$ ), the increase of the concentration of  $\text{CO}_3^{2-}$  makes the corrosion potential lower and the corrosion tendency higher. It also can be seen that all samples exhibit self-passivated characterization, translating directly into the passive region from the Tafel region. Polarization resistance exhibits a rapid drop as the concentration of  $\text{CO}_3^{2-}$  increases from  $0$  to  $1.5\text{ g/L}$ ; however, the anodic current basically remains stable. This indicates that although the small amount of  $\text{CO}_3^{2-}$  weakened the corrosion-resistance capacity of TA2 in the brine,  $\text{CO}_3^{2-}$  can boost the formation of protective films on TA2 by reaction with  $\text{Mg}^{2+}$ ,  $\text{Ca}^{2+}$  to yield a layer of carbonate on TA2 surface [17]. As the concentration of  $\text{CO}_3^{2-}$  increases from  $1.5\text{ g/L}$  to  $3.5\text{ g/L}$ , the anodic current density increases, suggesting that excessive  $\text{CO}_3^{2-}$  may exacerbate the corrosion of TA2 in the brine solution. When the concentration of  $\text{CO}_3^{2-}$  continuously increased, the precipitation film depositing on the metal surface became loose and porous, which facilitates the adsorption of  $\text{Cl}^-$ , leading to the weakened corrosion resistance of the titanium sheet [18].

The Nyquist and Bode plots of TA2 in the brine with different concentrations of  $\text{CO}_3^{2-}$  are shown in Figure. 1c & d, respectively. The equivalent circuit diagram fitting the EIS results is illustrated in Figure. 2, where  $R_s$  is the solution resistance between the working electrode and the reference electrode;  $R_t$  is the charge transfer resistance;  $R_p$  is the film resistance of the passivation film on the TA2 surface. A constant phase element  $Q$  is placed to represent the double layer capacitance and passivation film

capacitance [19-20]. Zsimpwin software was used to fit the test data, and the CPE constant  $Y_0$  after fitting was converted into passivation film capacitance through formula (1) [21].

$$C = Y_0(\omega_n^n)^{n-1} \quad (1)$$

Where  $Y_0$  is the CPE constant;  $\omega_n^n$  is the frequency corresponding to the maximum of  $-z''$ ;  $n$  is the dispersion effect index. The fitting results are shown in Table 1.

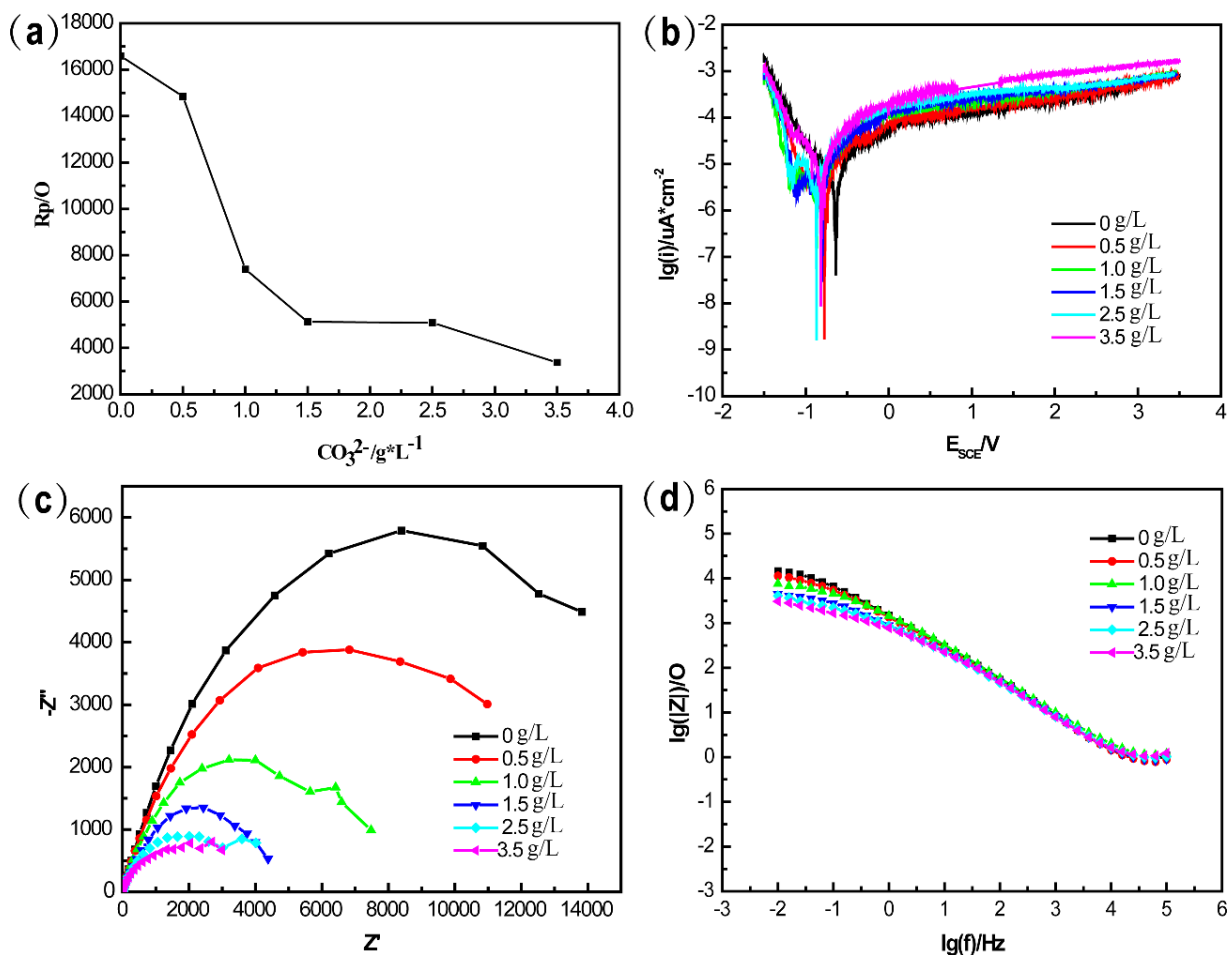


**Figure 1.** (a) Polarization resistance and (b) Potentiodynamic polarization curves, (c) Nyquist plots and (d) Bode plots for TA2 in the brine with different  $\text{CO}_3^{2-}$  concentrations.

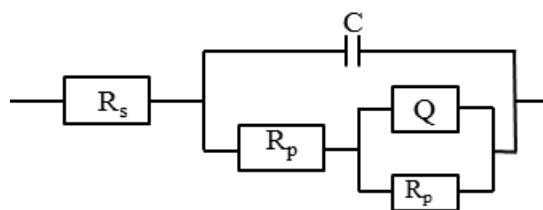


**Figure 2.** Equivalent circuit of TA2 in the brine with different  $\text{CO}_3^{2-}$  concentrations.

**Table 1.** Impedance fitting values of TA2 in the brine with different  $\text{CO}_3^{2-}$  concentrations

$\text{CO}_3^{2-}$ (g/L)	$R_s(\Omega/\text{cm}^2)$	$C(\mu\text{F}/\text{cm}^2)$	n	$R_p(\Omega/\text{cm}^2)$
0	0.9606	483.1	0.66	20030
0.5	0.8146	547.0	0.66	14070
1.0	1.084	554.5	0.66	7769
1.5	0.8744	721.5	0.61	5128
2.5	0.9834	801.7	0.59	4129
3.5	1.106	1754.9	0.54	3408

According to Figure. 1c & d, and Table 1, the increase of  $\text{CO}_3^{2-}$  concentration in the brine leads to the decrease of the capacitive reactance range and the dispersion coefficient. The rise of film capacitance indicates that the sediments deposited on the electrode surface grew gradually with the elevation of  $\text{CO}_3^{2-}$  concentration. The sediments can boost the charge holding capacity by absorbing water molecules, so formation of more sediments yielded the higher capacitance value [22].

When the surface of metal electrode is covered by passivation film in corrosive medium, the evolution of the passivation film mainly experiences the following three steps [23]: The first step is the process of metal ions leaving the lattice at the interface of metal/passivation film, which is not the control step of the whole process. The second step is the process of mass transfer through moving of metal ions in the passivation membrane from inside to outside. In the third step, a new passivation membrane or some complexes form at the passivation membrane/solution interface; simultaneously, the top layer of the passivation membrane and complexes on the surface may drop off into solution. The third process can be interpreted by equivalent resistance  $R_p$  ( $R_p$  is polarization resistance in linear polarization range). The bigger value of  $R_p$  means the better corrosion resistance of the material. The changes of  $R_p$  with the increase of  $\text{CO}_3^{2-}$  concentration in the brine (see Table 1) indicate that more  $\text{CO}_3^{2-}$  can weaken the resistance to uniform corrosion of TA2.

### 3.2 Influence of $\text{S}^{2-}$ on corrosion behavior of TA2

As shown in Figure 3a, when the concentration of  $\text{S}^{2-}$  in the brine increases from 0 to 0.2 g/L, the polarization resistance of TA2 drops significantly and then decreases slightly with the  $\text{S}^{2-}$  of 0.4–1.6 g/L. The free corrosion potential of TA2 exhibits a rapid negative shift, followed by a slow positive shift to a relatively stable value, and the anodic polarization current density increases with the addition of  $\text{S}^{2-}$  (Figure 3b), indicating that  $\text{S}^{2-}$  in the brine abated the resistance to uniform corrosion of TA2. It also can be seen that all samples present self-passivated characterization. The corrosion resistance of TA2 mainly depends on the protective effect of the passivation film on the surface. The highly electronegative  $\text{S}^{2-}$  adsorbed on the TA2 surface can prevent some beneficial substances ( $\text{O}_2$ ,  $\text{OH}^-$ , etc.) for the formation of metal passivation from approaching the metal surface, thus slowing down the growth rate of the passivation film [24]. No breakdown potential is observed in the range of potential test, which indicates that these passive films on the surface of TA2 are integral and protective.

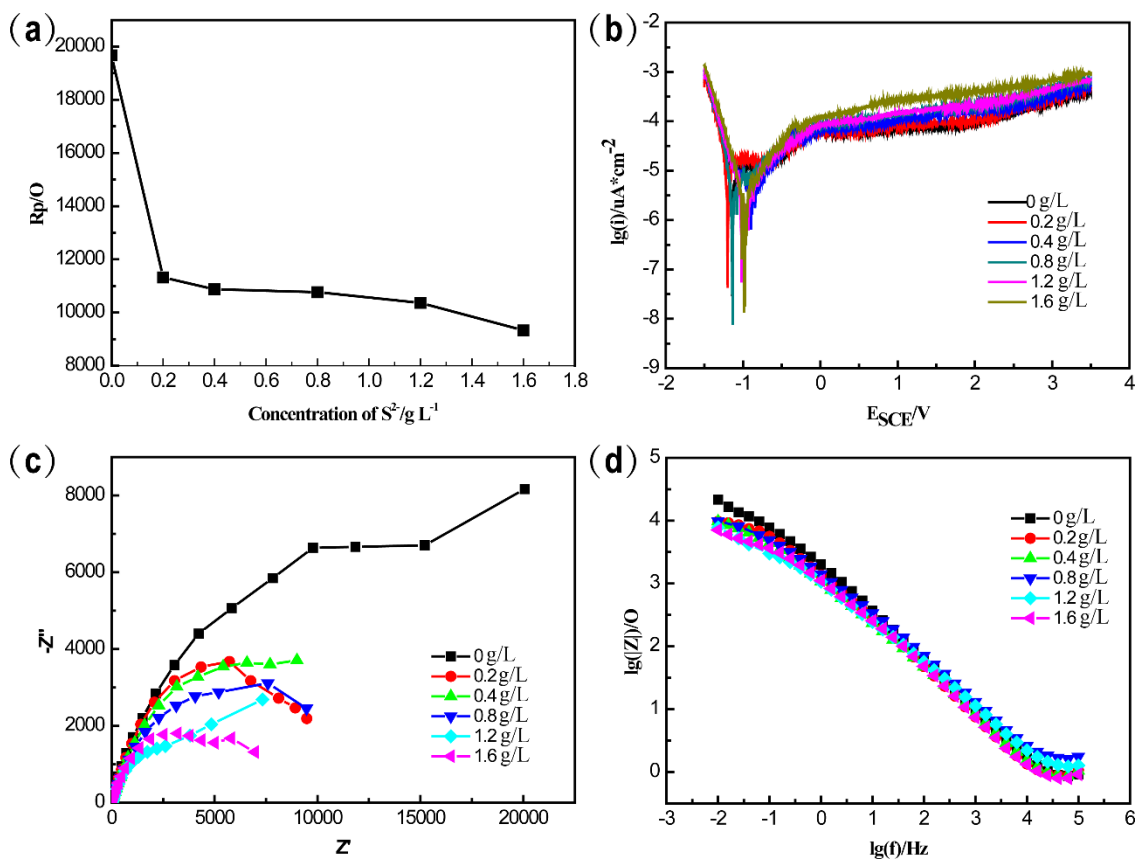


**Figure 3.** (a) Polarization resistance and (b) Potentiodynamic polarization curves, (c) Nyquist plots and (d) Bode plots for TA2 in the brine with different  $S^{2-}$  concentrations.

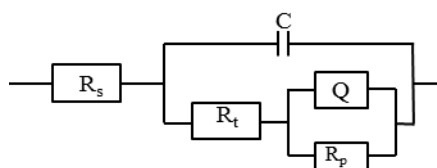


**Figure 4.** Equivalent circuit of TA2 in the brine with different  $S^{2-}$  concentrations

**Table 2.** Impedance fitting parameters of TA2 in the brine with different  $S^{2-}$  concentrations

$S^{2-}$ (g/L)	$R_s(\Omega/cm^2)$	$C(\mu F/cm^2)$	n	$R_p(\Omega/cm^2)$
0	0.8803	588.8	0.67	24560
0.2	0.9117	747.5	0.67	11710
0.4	0.8831	947.9	0.64	13720
0.8	1.5231	1069.9	0.63	12070
1.2	1.2421	1269.2	0.60	8894
1.6	0.8281	1343.6	0.61	7612

According to Figure 3c, d and Table 2, the elevation of  $S^{2-}$  concentration in the brine causes the decrease of capacitive reactance range and the increase of film capacitance, while the dispersion

coefficient first decreases and then basically stays unchanged with the rise of  $S^{2-}$  concentration. This phenomenon indicates that  $S^{2-}$  gradually accumulated on the electrode surface by adsorption process. Excess  $S^{2-}$  will accelerate the dissolution rate of passivation film and reduce the corrosion resistance of TA2 in brine [25-26]. The polarization resistance data in Table 2 demonstrate the resistance to uniform corrosion of TA2 decreases with the rise of  $S^{2-}$  concentration in the brine.

### 3.3 Influence of pH value on corrosion behavior of TA2

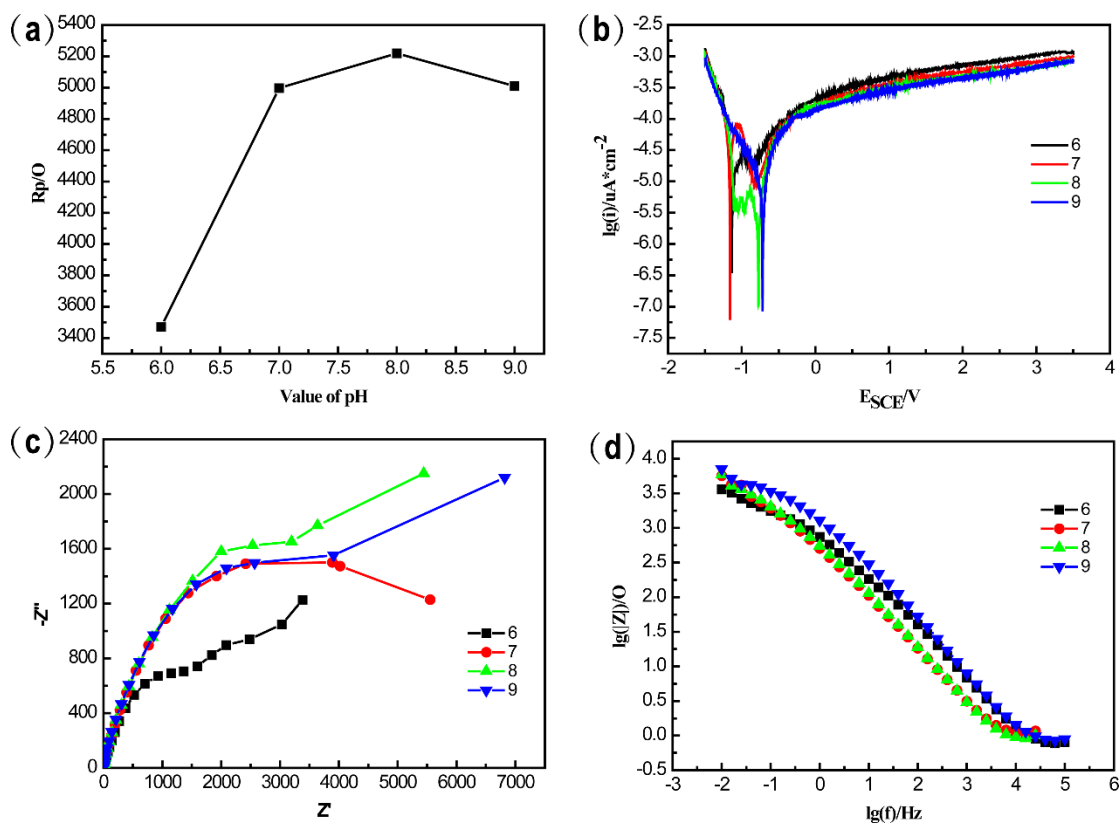


**Figure 5.** (a) Polarization resistance and (b) Potentiodynamic polarization curves, (c) Nyquist plots and (d) Bode plots for TA2 in the brine with different pH values.

pH value of solution can affect the corrosion behaviors of metals obviously. As shown in Figure 5a, in the acidic solution the polarization resistance of TA2 soars with the increase of pH value, and then the polarization resistance decreases at pH = 8. In the range of pH value (6 – 9), the higher free corrosion potential indicates the lower corrosion tendency, and the polarization curve decreases first and then increases (Figure 5b). As  $pH < 7$ , the  $H^+$  concentration in the brine increased with the decline of pH, leading to the dissolution of passivation film and subsequent decrease of the polarization resistance and rise of the self-corrosion rate. When the pH value was bigger than 7,  $O_2$  depolarizing reaction occurred on the cathode and metal oxidation reaction happened on the anode. Titanium ions can react with  $OH^-$  in the solution generating titanium oxide deposition on the metal surface, which can improve the corrosion resistance of the metal at a certain extent. At the same time, the breakdown potential was observed in the range of potential test at the pH value of 6–7. The corrosion breakdown potential is

about -76 mV. As the pH value continued to rise ( $\text{pH} > 8$ ),  $\text{CO}_3^{2-}$  in the brine could be converted into  $\text{HCO}_3^-$  partly, easily causing the inhomogeneity of the passivation film, making the corrosion potential of the metal negatively shift [27-28], resulting in weakening the corrosion resistance.

The Nyquist and Bode plots of TA2 in the brine solutions with different pH values are shown in Figure 5c & d. The curves diffuse in the low-frequency region of the impedance spectrum of which equivalent circuit diagram is illustrated in Figure 6. Accordingly, the relevant parameters were calculated and listed in Table 3. These results show that the raised pH value can reduce the capacitive reactance range; meanwhile the capacitance exhibits a change from decrease to increase. However, the diffusion coefficient undergoes an opposite trend compared with the capacitance. The dispersion coefficient always keeps the same trend as the pH changes. When the pH value of the solution is less than 7, the erosion effect of  $\text{Cl}^-$  is reinforced. As  $\text{pH} > 7$ , metal ions can combine with  $\text{OH}^-$  in solution to form oxide film or hydroxide oxide film (may be  $\alpha$ ,  $\beta$ -MOOH) [29], which can be deposited on the metal surface, improving the corrosion resistance of TA2. In addition, the active dissolution of metal is smaller in basic solution than in acidic one, and  $\text{OH}^-$  can compete with  $\text{Cl}^-$  for adsorption, which improves the pitting resistance of metal [30]. However, when the pH is too high, the passivation film on the metal surface may lose its stability, leading to the decline of the corrosion resistance of TA2 in the brine. Above results indicate that both the ranges of  $\text{pH} < 7$  and  $\text{pH} > 9$  can boost the corrosion of TA2 in the brine. So, it is crucial to choose an appropriate pH of the brine for relieving the corrosion of TA2.

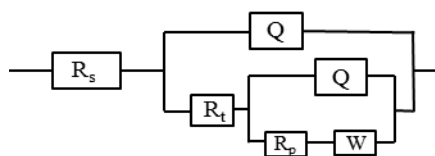


**Figure 6.** Equivalent circuit of TA2 in the brine with different pH values.

**Table 3.** Impedance fitting parameters of TA2 in the brine with different pH values

pH	$R_s(\Omega/\text{cm}^2)$	$C(\mu\text{F}/\text{cm}^2)$	n	$R_p(\Omega/\text{cm}^2)$	$W(\Omega/\text{cm}^2)$
6	0.6924	1627.9	0.56	2813	0.0029
7	1.0470	1151.6	0.63	5392	0.0042
8	0.8974	993.9	0.64	6027	0.0019
9	0.8666	1134.1	0.64	4903	0.0015

### 3.4 Influence of flow rate on corrosion behavior of TA2

In our previous research we have demonstrated the different corrosion behaviors of titanium in electrolyte with or without flowing. In this work, we utilized the same equipment as mentioned in the reference [10] to study the effects of different flow rates on the corrosion behaviors of TA2 in the brine solutions at 30 °C. As shown in Figure. 7a and 7b, with the increase of flow rate, the free corrosion

potential keeps stability. TA2 exhibits lower polarization resistance in the flowing brine than that in the stationary brine, indicating the flowing of solution weaken the corrosion resistance of TA2. The breakdown potential was observed in the brine without flowing. On the contrary in the flowing brine the breakdown potential disappeared, but samples still exhibited self-passivated characterization as translating directly into the passive region from the Tafel region.

The relatively lower flowing rate (<2 m/s) does not change the corrosion of TA2 obviously; however, the polarization resistance declines sharply at the flowing rate bigger than 2 m/s (Figure 7a), suggesting the higher flowing rate will accelerate the corrosion of TA2 in the brine. The Tafel curve (Figure 7b) measured in the flowing brine is unstable and fluctuates greatly due to the flowing of the brine, and all anodic polarization currents measured in the flowing brine are bigger than that in the stationary one. The anodic reaction of TA2 in the brine is the oxidation reaction with oxygen, and the oxygen molecules in the brine solution must diffuse through a retention layer on the metal surface to touch with the metal [31]. When the flowing rate was more than 2 m/s, the higher flowing rate reduced the thickness of the retention layer, facilitating the diffusion of oxygen molecules onto TA2, and then boosting the interaction between oxygen and TA2 [32].

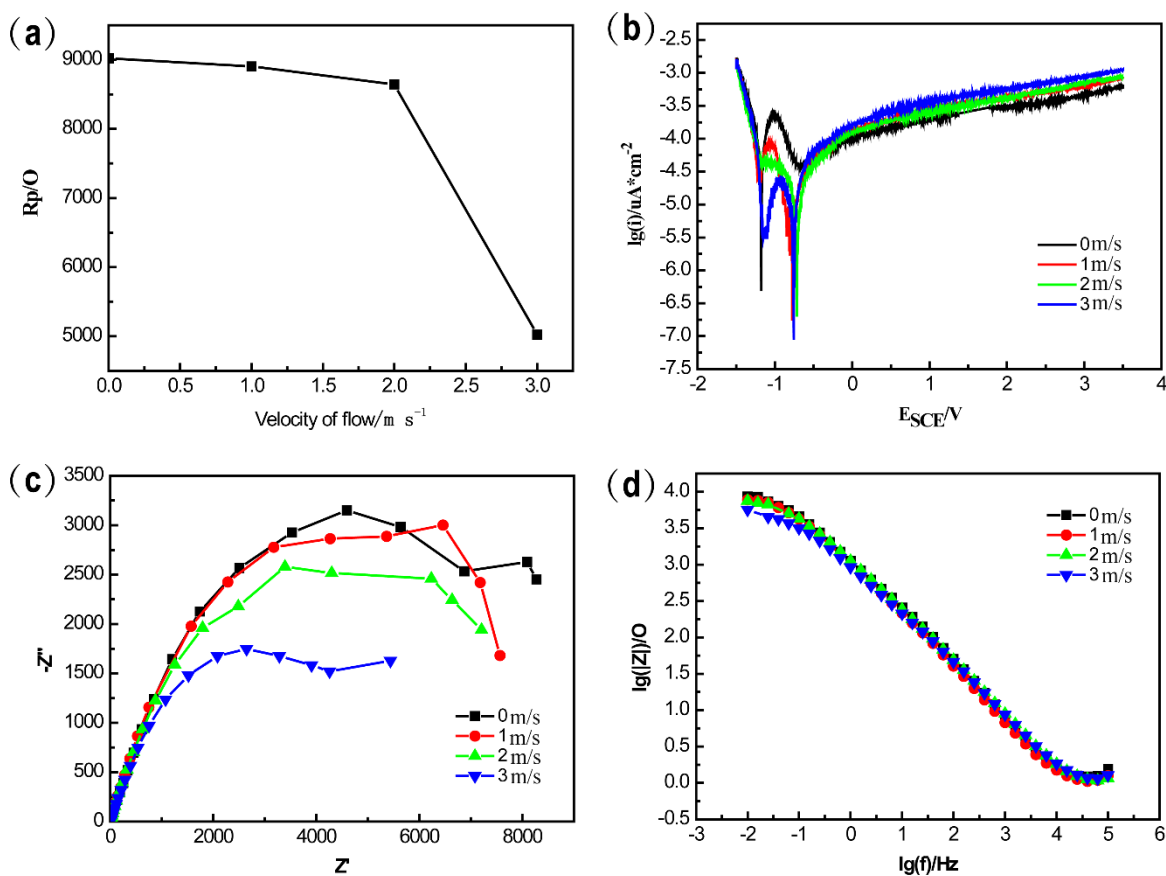


**Figure 7.** (a) Polarization resistance and (b) Potentiodynamic polarization curves, (c) Nyquist plots and (d) Bode plots for TA2 at the different flow rates of the brine.

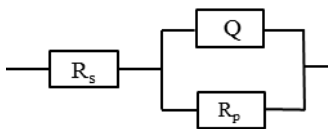


**Figure 8.** Equivalent circuit of TA2 in the brine at different flow rates.

**Table 4.** Impedance fitting parameters of TA2 in the brine at different flow rates

flowing rate(m/s)	$R_s(\Omega/cm^2)$	$C(\mu F/cm^2)$	n	$R_p(\Omega/cm^2)$
0	0.8818	406.1	0.72	12650
1	0.8426	426.5	0.74	8688
2	0.8864	433.9	0.73	8037
3	0.923	554.9	0.71	6856

As shown in Figure 7c, increasing the flow velocity of the brine causes decrease of the capacitive reactance range while the capacitance and dispersion coefficient remain stable basically (according to the data listed in Table 4). For each flow rate, there is only a single capacitive arc and the arc radius declines with the elevation of flowing rate, indicating that the corrosion resistance of TA2 becomes worse as rise of the flowing rate. When the flowing rate is below 3 m/s, the curvatures of the reactive arcs exhibit no obvious changes suggesting that, at lower flowing rate, the changes of flowing rate did not cause the significant fluctuation of the corrosion resistance. The Bode diagram (Figure 7d) shows the impedance in the low frequency region reduces with the increase of the flow rate, and the impedance in the high frequency region is almost the same at the different flow rates. According to R(QR), the high frequency region reflects the capacitance reactance of the interface capacitance. The same impedance value at the different flowing rates indicates the flowing rate of the brine did not influence the interface capacitance of TA2 significantly. This may be owing to the flowing solution washing away the corrosion products on the metal surface, so the metal surface maintained a good consistency [33]. The polarization resistance data in Table 4 also illustrate that increasing of the flowing rate of the brine will weaken the corrosion resistance of TA2.

### 3.5 orthogonal experiment results and analysis

According to the orthogonal test design level table of  $L_{16}(4^5)$ , the measured polarization resistance is shown in Table 5.

The order of the influence on the polarization resistance by different factors is as follows:  $A > C > B > D$ , which means that  $CO_3^{2-}$  concentration has the greatest influence on the corrosion of TA2 in the brine, and the flowing rate shows the least influence. The optimal parameter is A1B1C3D3, that is, 0 g/L of  $CO_3^{2-}$ , 0.8 g/L of  $S^{2-}$ , 8 of pH value and 2 m/s of flowing rate endows TA2 the best corrosion resistance. Consequently, to make TA2 better corrosion resistance in brine, the lower concentration of  $CO_3^{2-}$  is essential, and the pH value should be controlled between 7 and 8. The other factors can be adjusted according to the production requirements.

**Table 5.**  $L_{16}(4^5)$  orthogonal design table and processing results

No.	A	B	C	D	$R_p(\Omega)$
1	1	1	1	1	18198
2	2	1	2	2	31772
3	3	1	3	3	13002
4	4	1	4	4	11208
5	1	2	2	3	11200
6	2	2	1	4	9296
7	3	2	4	1	15418
8	4	2	3	2	13453
9	1	3	3	4	40594
10	2	3	4	3	30621
11	3	3	1	2	5316
12	4	3	2	1	12221
13	1	4	4	2	36435
14	2	4	3	1	19374
15	3	4	2	4	8205
16	4	4	1	3	16277
K1	106427	74180	49087	65211	
K2	91063	49367	63398	86976	
K3	41941	88752	86423	71100	
K4	53159	80291	93682	69303	
R	64486	39385	44595	21765	

#### 4. CONCLUSION

In the vacuum salt industry, titanium and its alloy have been used widely. The corrosion of titanium in the brine should be considered carefully for the safety and stable running of the water evaporation and salt formation. Herein the influences of multiple factors of the brine solution on the corrosion of titanium sheet have been evaluated. The relevant results indicate that the rise of  $\text{CO}_3^{2-}$  or  $\text{S}^{2-}$  will weaken the resistance to uniform corrosion of TA2 in the brine; the pH value of about 8 can make TA2 maintain good corrosion resistance. With the increase of the brine-flowing velocity, the corrosion resistance of TA2 will decrease. The optimum combination of these factors for the best corrosion resistance was achieved by the orthogonal experiment, and the results point that to make TA2 have better corrosion resistance in brine, the lower concentration of  $\text{CO}_3^{2-}$  and the pH = 7–8 should be guaranteed.

#### ACKNOWLEDGMENT

This work was supported by Sichuan province Key Laboratory of Vanadium and Titanium Resources Comprehensive Utilization(2018FTSZ06); the Opening Project of Material Corrosion and Protection Key Laboratory of Sichuan Province(2014CL20).

#### References

1. S. d. Wei, Y. F. Wei, T. Chen, C. B. Liu, Y. H. Tang, *Chem. Eng. J.*, 379(2020) 122407.

2. F. Nagies, K.E. Heusler, *Electrochim. Acta*, 43(1997) 41.
3. S. D. Hill, R. V. Mrazek, *Metall. Mater. Trans. B*, 5(1974) 53.
4. M. I. Abdulsalam, *J. Mater. Eng. Perform.*, 16(2007) 736.
5. C. P. Ernst, G. Cortain, M. Spohn, G. Rippin, B. W. Shausen, *Dentl. Mater.*, 18(2002) 351.
6. D. S. Kong, Y. Y. Feng, *J. Electrochem. Soc.*, 156(2009) 283.
7. R. Shah, D. S. Penmetsa, R. Thomas, D. S. Mehta, *Eur. J. Prosthodont. Re.*, 24 (2016) 171.
8. D. C. Rodrigues, P. Valderrama, Jr. Wilson, T. G. Palmer, *Materials*, 6(2013)5258.
9. J. Pang, D. J. Blackwood, *Corros. Sci.* 105 (2016) 17.
10. X.D. Chen, Q.S. Fu, Y.Z. Jin, M.T. Li, R.S. Yang, *Mat. Sci. Eng. C-Mater.*, 70 (2017) 1071.
11. P. Hu, R. Song, X. J. Li, J. Deng, Z. Y. Chen, Q. W. Li, K. S. Wang, W. C. Cao, D. X. Liu, H. L. Yu, *J. Alloy. Compd.*, 708 (2017) 367.
12. Z. B. Wang, H. X. Hu, C. B. Liu, Y. G. Zheng, *Electrochem. Acta*, 135 (2014) 526.
13. S. F. Zhao, H. G. Jia, J. H. Wang, *A.M. M.*, 99(2014)169.
14. A. Kawashima, S. Watanabe, K. Asami, S. J. Hanada, *Mater. Trans.*, 44 (2003) 1405.
15. K. A. D. Souza, A. Robin, *Mater. Chem. Phys.*, 103(2007) 351.
16. V. A. Levin, N. B. Kalinicheva, L. P. Chernykh, *Chem. Petrol. Eng.*, 12 (1976) 245.
17. J. G. Wang, H. Gao, *Adv. Mat. Res.*, 468 (2012) 1702.
18. Y. Bai, X. Gai, S. Li, L. C. Zhang, Y. Liu, Y. Hao, X. Zhang, R. Yang, Y. Gao, *Corros. Sci.*, 123 (2017) 289.
19. H. Sun, S. Liu, L. Sun, *Int. J. Electrochem. Sci.*, 8 (2013) 3494..
20. A. Y. Shenouda, K. R. Murali, *J. Power Sources*, 176 (2008) 332.
21. C. H. Hsu, F. Mansfeld, *Corrosion*. 57 (2001) 747.
22. S. L. Wu, Z. D. Cui, F. He, *Mater. Lett.* ,58 (2004) 1076.
23. S. Q. Chen, P. Wang, D. Zhang, *Mater. Des.*, 100 (2016) 254.
24. T. Li, J. Wu, G. S. Frankel, *Corros. Sci.*, 182 (2021) 109277.
25. M. Zhu, Q. Zhang, Y. F. Yuan, S. Y. Guo, *Int. J. Min. Met. Mater.*, 27 (2020) 1100.
26. R. Ion, S. Drob, M. Ijaz, C. Vasilescu, P. Osiceanu, D. Gordin, A. Cimpean, T. Gloriant, *Materials*, 9 (2016) 818.
27. S. Liu, H. Sun, L. Sun, H. Fan, *Corros. Sci.*, 65 (2012) 520.
28. X. Fu, W. Ma, S. Duan, Q. Wang, J. Lin, *Materials*, 12 (2019) 2614.
29. A. Y. Adesina, Z. M. Gasem, A. M. Kumar, *Metall. Mater. Trans. B*, 48 (2017) 1321.
30. H. Wei, Y. Wei, L. Hou, N. Dang, *Corros. Sci.*, 111 (2016) 382.
31. G. C. Pathiraja, N. Nanayakkara, A. Wijayasinghe, *B. Mater. Sci.*, 39 (2016) 803.
32. N. Oliveira, A. Guastaldi, *Acta Biomate.*, 5 (2009) 399.
33. D. Asefi, M. Arami, N. M. Mahmoodi, *Corros. Sci.*, 52 (2010) 794.